

# We are IntechOpen, the world's leading publisher of Open Access books Built by scientists, for scientists

4,800

Open access books available

122,000

International authors and editors

135M

Downloads

Our authors are among the

154

Countries delivered to

TOP 1%

most cited scientists

12.2%

Contributors from top 500 universities



WEB OF SCIENCE™

Selection of our books indexed in the Book Citation Index  
in Web of Science™ Core Collection (BKCI)

Interested in publishing with us?  
Contact [book.department@intechopen.com](mailto:book.department@intechopen.com)

Numbers displayed above are based on latest data collected.  
For more information visit [www.intechopen.com](http://www.intechopen.com)



---

# Improved Reduced Order Mechanical Model and Finite Element Analysis of Three-Dimensional Deformations of Epithelial Tissues

---

Ara S. Avetisyan, Asatur Zh. Khurshudyan and  
Sergey K. Ohanyan

Additional information is available at the end of the chapter

<http://dx.doi.org/10.5772/65027>

---

## Abstract

In this chapter, we analyse non-uniform bending of single-layer cell tissues—epithelia, surrounding organs throughout the body. Dimensionally reduced model is suggested, which is equivalent to membranes with bending stiffness: the total elastic energy of the tissue is a combination of stretching and bending energies. The energy, suggested in this chapter, is a piecewise function, the branches of which correspond to a specific deformation regime: compression, pure bending and stretch.

Under specific assumptions on a single cell, such as all cells are identical, elastic, homogeneous, have the shape of a hexagonal prism, are linked to each other by pure elastic junctions, and so on, tissues of different shapes are analysed using finite element discretization. The deformation of initially flat, cylindrical and spherical tissues is visualized to reproduce similar deformations in real epithelial tissues observed during experiments.

**Keywords:** morphogenesis, embryonic tissue, adherens junctions, relaxation, quasi-convex energy densities, isometric deformations, short maps, tissue mechanics,  $\Gamma$ -convergence, lower semi-continuity, hexagonal elements

---

## 1. Introduction

Morphogenesis, the evolutionary process of shape and structure development of organisms or their parts, is driven by certain types of cell shape changes or, in other words, deformations.

---

One type of such deformations is the apical constriction—visible shrinkage of the apical side of cells, leading to bending of epithelia—cell sheets, which surround organs throughout the body. First occurring at early stages of embryogenesis, the apical constriction results initially flat epithelia to be bent obtaining three-dimensional form, which, depending on physiological context and morphogenetic stage, leads to different consequences. It has been first hypothesized in [1] that in various developmental systems the apical constriction may drive the bending of epithelia. Using bulky mechanical construction, the hypothesis of Rhumbler is first practically tested in [2]. The testing mechanism consists of 13 identical bars (cell walls) that are kept apart by means of stiff tubes connecting their centres (cell kernels), and are held in a row by rubber bands connecting their ends (cell membrane). In the first stage, the rubber bands at both sides are stretched equally and the mechanism is in straight equilibrium. Shortening the rubber bands at, for instance, the upper side uniformly in each segment (cell), the mechanism is bent on the side of the greater tension, as it could be expected. Thus, Rhumbler's hypothesis could take place.

A more illustrative, computer model for verifying Rhumbler's hypothesis is suggested in [3], where bars and bands are replaced by virtual cells. Prescribing certain mechanical properties to the cell membrane and cytoplasmic components, and assuming that as a result of deformations the volume of a single cell is preserved, which is implicitly done by Rhumbler and Lewis, a model of cuboidal epithelia folding is suggested, based on the local behaviour of individual cells. The model is demonstrated on the example of ventral furrow formation in *Drosophila*. A sequence of cells in the form of a cylindrical shell, representing the cross section of ventral furrow, is deformed such that apical constriction occurs in its lower row of cells. Increasing the applied stresses, different steps of the furrow formation are illustrated. **Figure 1** expresses how much Odell's model is close to the real microscopic picture [4].

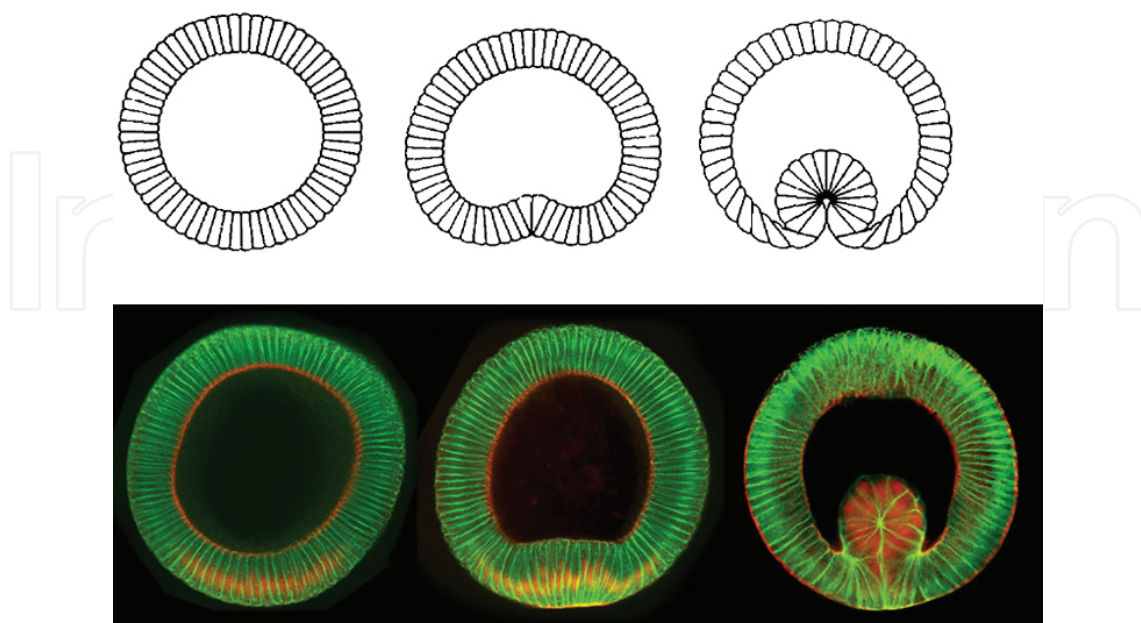


**Figure 1.** Ventral furrow formation in *Drosophila* according to [3] (upper) and [4] (lower).

Much is known about the causes of the apical constriction, but some issues still remain unexplored [5–8]. The most studied causes include contraction of actin filaments—fibrous network localized at the cortex of the cell, by interacting with motor protein myosin—the most known converter of chemical energy into mechanical work. Under influence of myosin, actin fibres contract leading to shrinkage of the cell in the area of their localization [9, 10]. The contraction size and principal direction of the fibres, that is, the microscopical deformation of a single cell, mainly depend on the tissue type: actin-myosin network contraction may deform columnar (occurring, for instance, in digestive tract and female reproductive system) or cuboid (resp. in kidney tubules) cells into trapezoidal-, wedge- or bottle-shaped cells. The deformation size strongly depends also on the emplacement of deforming cells: cells with different placement are constricted differently, so that macroscopically one observes localized wrinkles (see **Figure 2**).

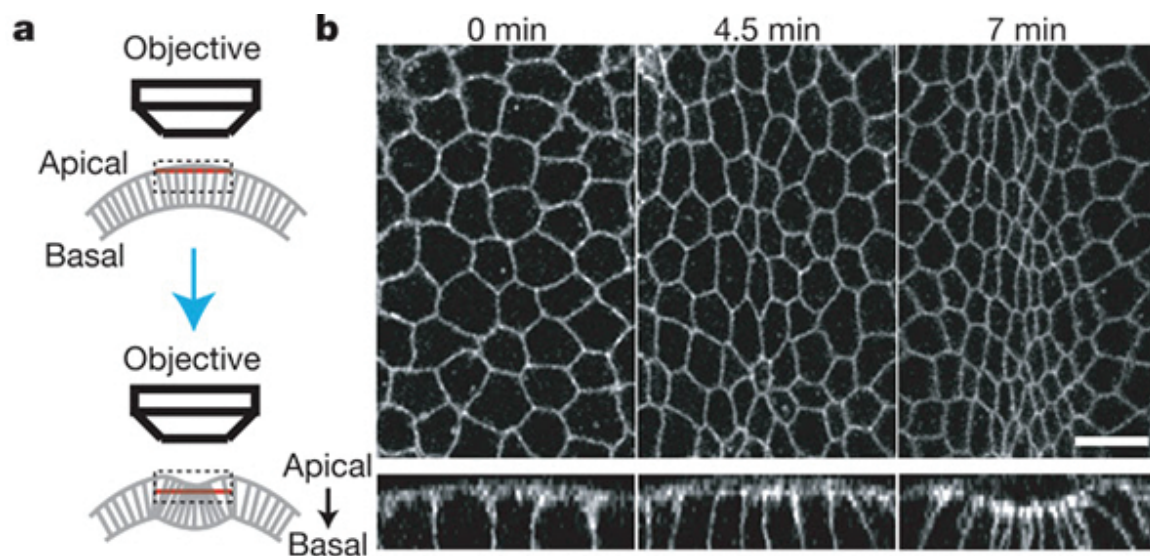


**Figure 2.** Apical constriction of ventral furrow at different times [10].

Because of the mechanical nature of cell shape change, in particular, apical constriction, its theoretical study first of all must rely on mechanical principles and constitutive laws. In early mechanical models, the tissue is modelled as a continuum material, so that the position and behaviour of individual cells are unimportant, that is, only macroscopic deformation of the tissue is studied. Moreover, the height of the cells (viz. the thickness of the tissue) is supposed to be negligible with respect to other measures, such that the deformation of the tissue can be described in terms of its mid-surface. In such models, the actin network is not explicitly accounted and the contraction forces are modelled as a force term acting on the outer surface of the epithelium. The actin network is explicitly accounted in [11], where thin elastic shell model based on linear Cauchy relations is derived to describe apical constriction in initially non-flat epithelia. The model is tested to simulate apical constriction in initially flat, cylindrical and spherical tissues. Ventral furrow formation in *Drosophila* is simulated (see **Figure 3**), and it becomes evident from comparison of **Figures 1** and **3** that the model, being three-dimen-



sional, is in good correspondence with that from [3]: **Figure 1** corresponds to cross section of cylindrical shell from **Figure 3**. However, it does not involve the behaviour of individual cells and describes only macroscopic deformation. For further introduction into other mechanical models, we refer to [11–26].



**Figure 3.** Ventral furrow formation in *Drosophila* according to [11].

The physical and geometrical characteristics of individual cells are taken into account by mechanical model suggested in [27] describing three-dimensional deformations of cell sheet. Both actin-myosin network contractile tensions and cell-cell adhesion stresses are involved to contribute in epithelial tissue bending. Prescribing specific mechanical characteristics to cytoplasmic components and to the kernel, the effective energy of a cell, which is assumed to be a hexagonal prism with constant volume, is expressed in terms of its basal length. As a result of simulations, it is particularly established that when adhesion stresses, distributed on lateral sides of the cell, are large enough, the effective energy has two local minima, that is, there are two equilibrium cell shapes. More particular, depending on position, cell shape may be discontinuously transited from squamous to columnar forms. **Figure 4** shows that there is a whole domain in the plane of lateral adhesion and actin-myosin tensions for which the effective energy has two local minima.

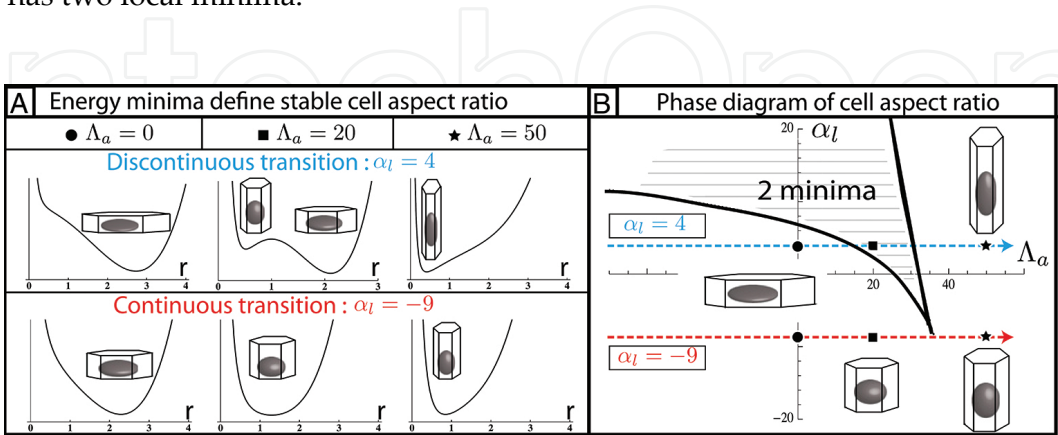


**Figure 4.** Epithelial cell aspect ratio as a bistable phenomenon [27]:  $\alpha_l$  is the contractile force and  $\Lambda_a$  is the actin-myosin tension.

In mathematical terms, it means that the total energy of the tissue is not *lower semi-continuous*, which implies that there is no convergence of its minimizers, and, therefore, it becomes impossible to derive real deformation of the tissue [28, 29]. To be more illustrative, consider a membrane, that is, a tissue without bending stiffness, which is compressed by boundary stresses. The only way that the membrane can accommodate a compressed state is due to *wrinkling* [30]. Wrinkles may occur more and more finely, so the limiting deformation will be smooth, but evidently it will not minimize the membrane energy.

To overcome such difficulties, the membrane energy density is usually substituted by its *quasi-convex envelope* [28], which ensures the lower semi-continuity of its total energy. In calculus of variations, there are several ways to construct or even compute convex envelopes for functionals, depending on first- and second-order derivatives [28, 31–36].

Another possibility for incorporating the lack of lower semi-continuity of membrane energy functionals is accounting the bending stiffness of the membrane and adding to the energy the bending contribution [37]. So, it is established in [33, 34] that the total energy of a membrane with some bending stiffness and thickness  $h$ , that is, the functional

$$E[\mathbf{r}] = hE_m[\mathbf{r}] + h^3E_b[\mathbf{r}] \quad (1)$$

of deformation  $\mathbf{r}$  consisting of membrane ( $E_m$ ) and bending ( $E_b$ ) contributions is lower semi-continuous for arbitrary  $E_m$  as far as  $E_b$  is lower semi-continuous. Explicit forms for  $E_m$  and  $E_b$  as well as sufficient conditions on material constants for which  $E_b$  (and therefore  $E$ ) is lower semi-continuous are derived *ibid*. Such materials are called *stable*.

However, the most rigorous and general approach seems to be the derivation of low-order energies from general three-dimensional non-linear elasticity by means of  $\Gamma$ -convergence. The concept was originally developed by De Giorgi, see [29]. It turns out that the  $\Gamma$ -limit of three-dimensional elastic energy functional, when the thickness of the body goes to zero, is always lower semi-continuous and since most commonly used two-dimensional energy functionals, that is, membrane energy, pure bending (Kirchhoff) energy and higher-order terms (von Kármán-like energies), are already derived as such limits (see Section 3), it becomes possible to analyze real deformations of particular tissues.

By suggested improvements, it is supposed to get rid of disadvantages of previous models and take into account the fact that the total energy of the tissue can have two local minima. Thus, we are intended

- to account the height of each individual cell, so the model is fully three-dimensional,
- to pick up strongly localized internal forces to model the phenomenon of apical constriction more precisely,
- to introduce stretching and bending contributions into the total elastic energy of the epithelial tissue, thus making the model more realistic and convenient not only for qualitative but also for quantitative analysis,

- to use the quasi-convexification of the total energy, so the real three-dimensional deformations of the epithelial tissues can be identified as minimizers of the total energy by a gradient flow technique.

The former allows making simplified toolboxes for analysing three-dimensional deformations of epithelial tissues. The rough diagram of the improved model looks like in **Figure 5**, so that the characteristics of each individual cell are important, as well as the actin belt is explicitly involved in the model.

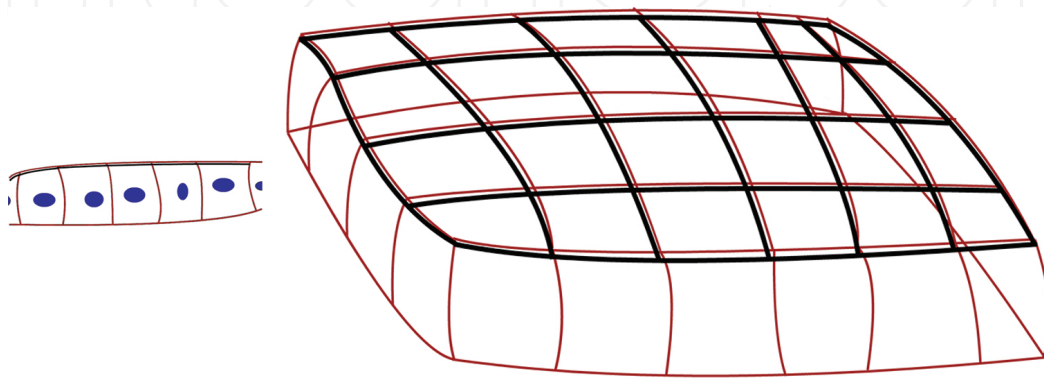


**Figure 5.** Diagrams of a single-cell layer: cross section (left) and 3D shape (right).

The chapter is organized as follows: In Section 2, some preliminary definitions and main notations are brought to make the chapter independent of outer sources. In Section 3, known results from  $\Gamma$ -convergent energies are shortly described. In Section 4, the quasi-convex envelope of membrane energy densities of general form is derived explicitly and sufficient conditions for their convexity are derived. Moreover, a specific energy is suggested for different deformation regimes that fully satisfies the needs of basic mechanical theory suggestion. Finally, in Section 5 main results of finite element analysis of tissues of particular initial shapes (flat, cylindrical, spherical) are discussed. Overall conclusion completes the body of the chapter.

## 2. Preliminaries

We begin with the definition of concepts used throughout the paper, which and much more on this topic can be found in [28, 29].

There are different concepts of convexity in higher dimensions, such as *quasi*-, *poly*-, *rank-one* and *separately convexity*. Here, we use all but poly-convexity, so it is of no use to enlarge the chapter by its definition.

**Definition 1** (quasi-convexity). A function  $W : \mathbb{R}^{N \times n} \rightarrow \mathbb{R} \cup \{+\infty\}$  is said to be *quasi-convex* if

$$W(\mathbf{G}) \leq \frac{1}{\mu(\Omega)} \int_{\Omega} W(\mathbf{G} + \nabla \mathbf{r}_0(\mathbf{x})) d\mathbf{x}, \quad (2)$$

for every bounded open set  $\Omega$ , for every  $\mathbf{G} \in \mathbb{R}^{N \times n}$  and for every  $\mathbf{r}_0 \in W_0^{1,p}(\Omega, \mathbb{R}^N)$ .

**Definition 2** (rank-one convexity). A function  $W : \mathbb{R}^{N \times n} \rightarrow \mathbb{R} \cup \{+\infty\}$  is said to be rank-one convex if

$$W(\mathbf{G} + \theta \mathbf{F}) \leq (1 - \theta)W(\mathbf{G}) + \theta W(\mathbf{G} + \mathbf{F}), \quad (3)$$

for every  $\theta \in [0, 1]$ ,  $\mathbf{G}, \mathbf{F} \in \mathbb{R}^{N \times n}$  with  $\text{rank } \mathbf{F} = 1$ .

**Definition 3** (separately convexity). A function  $W : \mathbb{R}^N \rightarrow \mathbb{R} \cup \{+\infty\}$  is said to be separately convex if

$$W(x_1, \dots, x_{i-1}, x_i, x_{i+1}, \dots, x_N) \quad (4)$$

is convex for every  $i = 1, \dots, N$  and for every fixed  $(x_1, \dots, x_{i-1}, x_{i+1}, \dots, x_N) \in \mathbb{R}^{N-1}$ .

In other words, a function  $W : \mathbb{R}^N \rightarrow \mathbb{R} \cup \{+\infty\}$  is separately convex if it is convex on every line parallel to a coordinate axis.

In general, convexity implies quasi-convexity, which implies rank-one convexity, and finally rank-one convexity implies separately convexity.

The quasi-convexity notion is generalized by Meyers [38] for functionals depending on higher-order derivatives. We refer to [32, 35, 36] for practical use of the definition.

**Definition 4** ( $k$ -quasi convexity). A function  $W : \mathbb{R}^{N \times n} \rightarrow \mathbb{R} \cup \{+\infty\}$  is said to be  $k$ -quasi-convex if

$$W(\mathbf{G}) \leq \frac{1}{\mu(\Omega)} \int_{\Omega} W(\mathbf{G} + \nabla^k \mathbf{r}_0(\mathbf{x})) d\mathbf{x}, \quad (5)$$

for every open-bounded set  $\Omega$ , for every  $\mathbf{G} \in \mathbb{R}^{N \times n \times k}$  and for every  $\mathbf{r}_0 \in W_0^{k,p}(\Omega, \mathbb{R}^N)$ .

In particular, 2-quasi-convex functions, which we use here, are the restriction of quasi-convex functions to symmetric matrices [39] (in the case of  $k$ -quasi convexity, see [40]).

We widely use the quasi-convex envelope of  $W(\mathbf{G})$  or *apparent energy density*,  $W_q(\mathbf{G})$ , which can be defined in terms of deformations of the form  $\mathbf{r}(x) = \mathbf{G}x + \mathbf{r}_0(x)$  with  $\mathbf{G} \in \mathbb{R}^{N \times n}$  constant,  $x \in \mathbb{R}^n$  and  $\mathbf{r}_0(x) = 0$  on the boundary  $\partial\Omega$  [41, 42]:

$$W_q(\mathbf{G}) = \frac{1}{\mu(\Omega)} \inf_{\mathbf{r}_0|_{\partial\Omega}=0} \int_{\Omega} W(\mathbf{G} + \nabla \mathbf{r}_0) d\mathbf{x}. \quad (6)$$

It is evident that for any  $\mathbf{G} \in \mathbb{R}^{N \times n}$ ,  $0 \leq W_q \leq W$ , and when  $W = 0$ ,  $W_q = 0$  as well.

Deformation is always denoted by  $\mathbf{r} : \Omega \rightarrow \mathbb{R}^3$  with open-bounded  $\Omega \in \mathbb{R}$ . We introduce the first and second fundamental forms of a deformation  $\mathbf{r}$

$$\mathbf{I} = (\nabla \mathbf{r})^T \nabla \mathbf{r}, \quad \mathbf{II} = \left\{ \frac{\partial^2 \mathbf{r}}{\partial x_i \partial x_j} \cdot \mathbf{n} \right\}_{i,j=1,2}, \quad (7)$$

respectively, in which  $\mathbf{n} = \frac{1}{\left| \frac{\partial \mathbf{r}}{\partial x_1} \times \frac{\partial \mathbf{r}}{\partial x_2} \right|} \frac{\partial \mathbf{r}}{\partial x_1} \times \frac{\partial \mathbf{r}}{\partial x_2}$  is the unit of the outer normal to  $\Omega$ . The first fundamental form quantitatively characterizes the stretch or compression of the membrane, while the second fundamental form characterizes its curvature.

**Definition 5.** Energy density function  $W : \mathbb{R}^{3 \times 2} \rightarrow \mathbb{R}^2$  is called frame indifferent if for all rotations  $\mathbf{R}_3 \in \text{SO}(3)$

$$W(\mathbf{R}_3 \mathbf{G}) = W(\mathbf{G}). \quad (8)$$

If for all  $\mathbf{R}_2 \in \text{SO}(2)$ ,

$$W(\mathbf{G} \mathbf{R}_2) = W(\mathbf{G}), \quad (9)$$

then it is called isotropic.

In other words, frame indifferent energy densities are invariant against three-dimensional rotations before a deformation is applied and that isotropic energy densities are invariant against two-dimensional rotations after a deformation is applied.

**Definition 6** (short ( $\delta$ -short) deformation). A deformation  $\mathbf{r} : \Omega \rightarrow \mathbb{R}^3$  is called short ( $\delta$ -short) if  $\mathbf{I}(\nabla \mathbf{r}) \leq \text{Id}_2 \times 2$  ( $\leq \delta \text{Id}_2 \times 2$ ) a.e. in  $\Omega$ .

**Definition 7** (isometric deformation). A deformation  $\mathbf{r} : \Omega \rightarrow \mathbb{R}^3$  is called isometric if  $\mathbf{I}(\nabla \mathbf{r}) = \text{Id}_2 \times 2$  a.e. on  $\Omega$ .

Short deformations result compressive stresses, while isometric deformations do not allow stretching or compression. The case  $\mathbf{I} \geq \text{Id}_2 \times 2$  corresponds to tensile or, in general, non-compressive stresses. It is known that for non-compressive stresses, the membrane energy density function is already quasi-convex [41, 42].



### 3. $\Gamma$ -convergence and $\Gamma$ -limits of three-dimensional non-linear elastic energy

Rigorous derivation of two-dimensional energy functionals for thin bodies from three-dimensional functionals is of particular interest. There are several ways for dimension reduction, such as asymptotic expansion,  $\Gamma$ -convergence technique, and so on (for general survey, see [43]). In [44], a hierarchy of plate models is derived as  $\Gamma$ -limit of three-dimensional elastic energy functional when the thickness of the body  $h \rightarrow 0$ . It turns out that the scaling of external force in  $h$  plays an important role for  $\Gamma$ -limit derivation. Suppose a body occupies the domain  $\Omega \times \left[-\frac{h}{2}, \frac{h}{2}\right]$ , and the applied forces  $\mathbf{f}^{(h)} : \Omega \rightarrow \mathbb{R}^3$  active on the outer surface of the body satisfy

$$\frac{1}{h^\alpha} \mathbf{f}^{(h)} \rightharpoonup \mathbf{f} \quad \text{in } L^2(\Omega, \mathbb{R}^3), \quad (10)$$

and

$$E^h[\mathbf{r}] = \frac{1}{h} E[\mathbf{r}] = \int_{\Omega \times \left(-\frac{1}{2}, \frac{1}{2}\right)} W(\nabla_h \mathbf{r}) dx \quad (11)$$

denotes the rescaled elastic energy of the body, with

$$\nabla_h \mathbf{r} = \left( \frac{\partial \mathbf{r}_1}{\partial x_1}, \frac{\partial \mathbf{r}_2}{\partial x_2}, \frac{1}{h} \frac{\partial \mathbf{r}_3}{\partial x_3} \right). \quad (12)$$

The total energy of the body will be

$$E^h[\mathbf{r}] = E^h[\mathbf{r}] - \int_{\Omega \times \left(-\frac{1}{2}, \frac{1}{2}\right)} \mathbf{f}^{(h)}(\mathbf{x}) \cdot \mathbf{r} dx. \quad (13)$$

The  $\Gamma$ -limit

$$\Gamma - \lim_{h \rightarrow 0} \frac{1}{h^\beta} E^h[\mathbf{r}] \quad (14)$$

for  $\beta \geq 0$  will provide constitutive mechanical models to analyse deformed three-dimensional shape of initially flat thin bodies.

We combine the results of [44–48] in Theorem 1.

**Theorem 1.** Let the stored energy density function is frame indifferent and satisfy

$$W = 0 \quad \text{on} \quad \text{SO}(3), \quad (15)$$

$$W(\mathbf{F}) \geq c \text{dist}^2(\mathbf{F}, \text{SO}(3)), \quad c > 0, \quad (16)$$

and in a neighbourhood of  $\text{SO}(3)$ ,  $W \in C^2$ .

Then

(i) (Membrane theory [45]). Suppose  $\alpha = \beta = 0$  and

$$W(\mathbf{F}) \leq C(1 + |\mathbf{F}|^p), \quad W(\mathbf{F}) \geq c|\mathbf{F}|^p - C, \quad p \geq 2, c > 0. \quad (17)$$

Then  $|\inf \mathcal{E}^h| \leq C$  is a  $\beta$ -minimizing sequence, that is, if

$$\limsup_{h \rightarrow 0} \frac{1}{h^\beta} [E^h[\mathbf{r}] - \inf E^h] = 0, \quad (18)$$

then  $\mathbf{r}^{(h)} \rightharpoonup \bar{\mathbf{r}}$  in  $W^{1,2} \left( \Omega \times \left( -\frac{1}{2}, \frac{1}{2} \right); \mathbb{R}^3 \right)$  (for a subsequence). The limiting deformation  $\bar{\mathbf{r}}$  is independent of  $x_3$  and minimizes

$$E_0^0[\mathbf{r}] = \int_{\Omega} [W_q(\nabla \mathbf{r}) - \mathbf{f} \cdot \mathbf{r}] d\mathbf{x} \quad (19)$$

among all  $\mathbf{r} : \Omega \rightarrow \mathbb{R}^3$ . For derivation of  $W_q$  from given  $W$  see Section 4 subsequently.

(ii) (Constrained membrane theory [46]). Suppose that  $0 < \alpha < \frac{5}{3}$  and  $\beta = \alpha$ . Then  $|\inf \mathcal{E}^h| \leq Ch^\beta$  and every  $\beta$ -minimizing sequence  $\mathbf{r}^{(h)}$  has a subsequence with  $\mathbf{r}^{(h)} \rightharpoonup \bar{\mathbf{r}}$  in  $W^{1,2} \left( \Omega \times \left( -\frac{1}{2}, \frac{1}{2} \right); \mathbb{R}^3 \right)$  in . The limit  $\bar{\mathbf{r}}$  is independent of  $x_3$  and minimizes

$$E_\alpha^0[\mathbf{r}] = \int_{\Omega} [-\mathbf{f} \cdot \mathbf{r}] d\mathbf{x} \quad (20)$$

among all short deformations  $\mathbf{r} : \Omega \rightarrow \mathbb{R}^3$ .

(iii) (Non-linear bending theory [47]). Suppose  $\alpha = \beta = 2$ . Then  $|\inf \mathcal{E}^h| \leq Ch^2$  and if  $\mathbf{r}^{(h)}$  is a  $\beta$ -minimizing sequence then there is strong convergence  $\mathbf{r}^{(h)} \rightarrow \bar{\mathbf{r}}$  in  $W^{2,2}(\Omega; \mathbb{R}^3)$  (for a subsequence). The

limiting deformation  $\bar{\mathbf{r}}$  is isometric, independent of  $x_3$ , belongs to  $W^{2,2}\left(\Omega \times \left(-\frac{1}{2}, \frac{1}{2}\right); \mathbb{R}^3\right)$  and minimizes

$$E_2^0[\mathbf{r}] = \int_{\Omega} \left[ \frac{1}{24} Q_2(\mathbf{\Pi}) - \mathbf{f} \cdot \mathbf{r} \right] d\mathbf{x} \quad (21)$$

among all isometric deformations  $\mathbf{r} : \Omega \rightarrow \mathbb{R}^3$ , which belong to  $W^{2,2}(\Omega; \mathbb{R}^3)$ . The non-linear strain satisfies

$$\frac{1}{h} \left[ \left( \nabla \mathbf{r}^{(h)} \right)^T \nabla \mathbf{r}^{(h)} - \text{Id} \right] \rightarrow x_3 (\mathbf{\Pi} + \text{sym } a_{\min} \otimes e_3), \quad (22)$$

where  $2 \text{sym } \mathbf{G} = \mathbf{G}^T + \mathbf{G}$ ,  $a_{\min}$  is the solution of

$$Q_2(\mathbf{G}) = \min_{a \in \mathbb{R}^3} Q_3(\mathbf{G} + a \otimes e_3 + e_3 \otimes a), \quad Q_3(\mathbf{G}) = \left. \frac{\partial^2 W}{\partial \mathbf{G}^2} \right|_{\mathbf{G} = \text{Id} = 0}. \quad (23)$$

In all cases, there is convergence of energy, that is,

$$\lim_{h \rightarrow 0} \frac{1}{h^\beta} E^h[\mathbf{r}^{(h)}] = \lim_{h \rightarrow 0} \frac{1}{h^\beta} \inf E^h = E_\alpha^0[\bar{\mathbf{r}}] = \min E_\alpha^0. \quad (24)$$

For  $\alpha > 0$ , the limiting deformation  $\bar{\mathbf{r}}$  is not only isometric but is close to a rigid motion. For that reason in [44], for deformation  $\mathbf{r}^{(h)} : \Omega \left( -\frac{1}{2}, \frac{1}{2} \right) \rightarrow \mathbb{R}^3$ , the deformation

$$\tilde{\mathbf{r}}^{(h)} = \left( \mathbf{R}^{(h)} \right)^T \mathbf{r}^{(h)} - \mathbf{c}^{(h)} \quad (25)$$

with  $\tilde{\mathbf{R}}^{(h)} \in \text{SO}(3)$  and  $\mathbf{c}^{(h)} \in \mathbb{R}^3$ , is introduced and the averaged in-plane and out-of-plane displacements

$$\mathbf{U}^{(h)}(x_1, x_2) = \int_{-\frac{1}{2}}^{\frac{1}{2}} \left[ \begin{pmatrix} \tilde{\mathbf{r}}_1^{(h)} \\ \tilde{\mathbf{r}}_2^{(h)} \end{pmatrix} (x_1, x_2, x_3) - \begin{pmatrix} x_1 \\ x_2 \end{pmatrix} \right] dx_3, \quad \mathbf{V}^{(h)}(x_1, x_2) = \int_{-\frac{1}{2}}^{\frac{1}{2}} \tilde{\mathbf{r}}_3^{(h)} dx_3 \quad (26)$$

are rescaled by

$$\mathbf{u}^{(h)} = \frac{1}{h^\gamma} \mathbf{U}^{(h)}, \quad \mathbf{v}^{(h)} = \frac{1}{h^\delta} \mathbf{V}^{(h)}, \quad (27)$$

respectively.

Then, we have

**Theorem 2.** (iv) (Linearized isometry constraint). Suppose  $2 < \alpha < 3$  and set  $\beta = 2\alpha - 2$ ,  $\gamma = 2(\alpha - 2)$ ,  $2\delta = \gamma$ . If  $2 < \alpha < \frac{5}{2}$ , suppose in addition that  $\Omega$  is simply connected. Then,  $-Ch^\beta \leq \inf \varepsilon^h \leq 0$ . If  $\mathbf{r}^{(h)}$  is a  $\beta$ -minimizing sequence then there exist constant  $\mathbf{R}^{(h)} \in \text{SO}(3)$  and  $c(h) \in \mathbb{R}^3$  such that

$$\mathbf{R}^{(h)} \rightarrow \bar{\mathbf{R}}, \quad (28)$$

$$\nabla_h \tilde{\mathbf{r}} \rightarrow \text{Id} \quad \text{in} \quad L^2 \left( \Omega \times \left( -\frac{1}{2}, \frac{1}{2} \right); \mathbb{R}^{3 \times 3} \right), \quad (29)$$

$$\mathbf{u}^{(h)} \rightarrow \bar{\mathbf{u}}, \quad \mathbf{v}^{(h)} \rightarrow \bar{\mathbf{v}}, \quad \text{in} \quad W^{1,2}(\Omega; \mathbb{R}^2), \quad \bar{\mathbf{v}} \in W^{2,2}(\Omega; \mathbb{R}^2), \quad (30)$$

$$\nabla \bar{\mathbf{u}} + (\nabla \bar{\mathbf{u}})^T + \nabla \bar{\mathbf{v}} \otimes \nabla \bar{\mathbf{v}} = 0. \quad (31)$$

Moreover, the pair  $(\bar{\mathbf{v}}, \bar{\mathbf{R}})$  minimizes the functional

$$E_{lin}^{vK}(\mathbf{v}, \mathbf{R}) = \int_{\Omega} \left[ \frac{1}{24} Q_2(\nabla^2 \mathbf{v}) - \mathbf{R}_{33} \mathbf{f}_3 \cdot \mathbf{v} \right] dx, \quad (32)$$

subject to  $\det \nabla^2 \mathbf{v} = 0$ .

(v) (von Kármán theory). Suppose that  $\alpha = 3$  and set  $\beta = 4$ ,  $\gamma = 2$ ,  $\delta = 1$ . Then  $-Ch^\beta \leq \varepsilon^h \leq 0$  and for a subsequence of a  $\beta$ -minimizing sequence, (1) and (2) hold and the limit triple  $(\bar{\mathbf{u}}, \bar{\mathbf{v}}, \bar{\mathbf{R}})$  minimizes von Kármán functional

$$\begin{aligned} E^{vK}(\mathbf{u}, \mathbf{v}, \mathbf{R}) &= \frac{1}{2} \int_{\Omega} \left[ Q_2 \left( \frac{1}{2} \left[ \nabla \mathbf{u} + (\nabla \mathbf{u})^T + \nabla \mathbf{v} \otimes \nabla \mathbf{v} \right] \right) + \frac{1}{24} Q_2(\nabla^2 \mathbf{v}) \right] dx - \\ &\quad - \mathbf{R}_{33} \int_{\Omega} \mathbf{f}_3 \cdot \mathbf{v} dx. \end{aligned} \quad (33)$$

(vi) (Linearized von Kármán theory). Suppose  $\alpha > 3$  and set  $\beta = 2\alpha - 2$ ,  $\gamma = \alpha - 1$  and  $\delta = \alpha - 2$ . Then  $-Ch^\beta \leq \inf \varepsilon^h \leq 0$  and for a sequence of a  $\beta$ -minimizing sequence. (2) holds with  $\bar{\mathbf{u}} = 0$  and the pair  $(\bar{\mathbf{v}}, \bar{\mathbf{R}})$  minimizes the linearized von Kármán functional

$$\varepsilon^{vK}(\mathbf{v}, \mathbf{R}) = \int_{\Omega} \left[ \frac{1}{24} Q_2(\nabla^2 \mathbf{v}) - \mathbf{R}_{33} \mathbf{f}_3 \cdot \mathbf{v} \right] d\mathbf{x}. \quad (34)$$

Moreover, the non-linear strain satisfies

$$\frac{1}{h^{1-\alpha}} \left( \left[ (\nabla_h \mathbf{r}^{(h)})^T \nabla_h \mathbf{r}^{(h)} \right]^{\frac{1}{2}} - \text{Id} \right) \rightarrow \text{sym } \mathbf{G}. \quad (35)$$

In all cases, we have convergence of the rescaled energy  $h^{-\beta} \mathcal{E}^h(\mathbf{r}^{(h)})$  to the minimum of the limit functional  $\mathcal{E}_\alpha^{vK}$ . Moreover, for  $\mathbf{f}_3 \neq 0$  we have  $\bar{\mathbf{R}}_{33} = 1$  or  $-1$ .

**Remark 1.** (i) Practically, Theorems 1 and 2 establish  $\Gamma$ -convergence and give the  $\Gamma$ -limits of three-dimensional non-linear energy functional in the range  $\beta \in [0, \frac{5}{3}) \cup [2, \infty)$ . The range  $\beta \in [\frac{5}{3}, 2)$  remains unexplored.

(ii) Even in the case  $\beta = \frac{5}{3}$ , it is still possible to find a sequence  $\mathbf{r}_k^{(h)}$  for which the functional  $h^{-\beta} \mathcal{E}^h[\mathbf{r}_k^{(h)}]$  is bounded when  $h \rightarrow 0$ . The limiting deformations  $\mathbf{r}$  are composed of finitely many affine isometries separated by sharp folds and are called origami deformations [46]. It is proved *ibid* that the class of origami deformations is the closure of the class of short deformations with respect to the uniform convergence.

(iii) In particular, when  $\alpha = \beta = 2$ , for isotropic homogeneous bodies we obtain

$$Q_2(\mathbf{\Pi}) = 2\mu |\mathbf{\Pi}|^2 + \frac{\lambda \cdot 2\mu}{\lambda + 2\mu} \text{tr}^2 \mathbf{\Pi}, \quad (36)$$

in which  $\lambda$  and  $\mu$  are Lamé constants, coinciding with plate energy derived by Kirchhoff much earlier in [49].



#### 4. Relaxation of epithelial elastic energy by Pipkin's procedure and by adding the bending contribution

As was mentioned in Section 1, there are two ways to relax the epithelial elastic energy. The first way is to relax the stretching energy for deformation regimes corresponding to compressive stresses. For that reason, Pipkin's procedure [41] seems to be the most common tool.

Suppose that the stretching energy density function  $W = W(\nabla \mathbf{r})$  is frame indifferent, isotropic and positive except the cases

$$\nabla \mathbf{r} = \begin{pmatrix} 1 & 0 \\ 0 & 1 \\ 0 & 0 \end{pmatrix} \text{ and } \nabla \mathbf{r} = \begin{pmatrix} \delta & 0 \\ 0 & \delta \\ 0 & 0 \end{pmatrix}, \quad 1 < \delta \in \mathbb{R}, \quad (37)$$

where it turns to zero, that is, attains its minimum. On elastic energies with two minima, see [50]. This assumption is motivated by bistability of cell shapes during apical constriction (see **Figure 4**).

We restrict attention to deformations  $\mathbf{r}$  with

$$\nabla \mathbf{r} = \begin{pmatrix} \sigma_1 & 0 \\ 0 & \sigma_2 \\ 0 & 0 \end{pmatrix}, \quad (38)$$

and denote  $W_q(\nabla \mathbf{r}) := \tilde{W}_q(\sigma_1, \sigma_2)$ . Here  $|\sigma_j| = \lambda_j$ ,  $j \in \{1; 2\}$ , are the principal stretches, the squares of which are the eigenvalues of the first fundamental form. Therefore

$$\lambda_{1,2}(\nabla \mathbf{r}) = \sqrt{\frac{1}{2} \left[ \text{tr}(\mathbf{I}(\nabla \mathbf{r})) \pm \sqrt{|\mathbf{I}(\nabla \mathbf{r})|^2 - 2 \det(\mathbf{I}(\nabla \mathbf{r}))} \right]}. \quad (39)$$

In view of frame indifference of  $W$ , and thence,  $\tilde{W}$ , we conclude that  $\tilde{W}_q(\pm \sigma_1, \pm \sigma_2) = \tilde{W}_q(\lambda_1, \lambda_2)$ .

From quasi-convexity of  $W_q$ , in particular, follows its rank-one convexity, therefore since the matrix

$$A = \begin{pmatrix} \delta_{11} & 0 \\ 0 & 0 \\ 0 & 0 \end{pmatrix}, \quad \delta_{11} \neq 0, \quad (40)$$

is rank one, we have

therefore  $\tilde{W}_q$  is convex with respect to  $\lambda_1$ . Repeating the argument when

$$A = \begin{pmatrix} 0 & 0 \\ 0 & \delta_{22} \\ 0 & 0 \end{pmatrix}, \quad \delta_{22} \neq 0, \quad (41)$$

we see that  $\tilde{W}_q(\lambda_1, \lambda_2)$  is separately convex.

Under assumptions made, we have  $\tilde{W}_q(\lambda_1, \lambda_2) = 0$  if  $\lambda_1 = \lambda_2 = 1$  and  $\lambda_1 = \lambda_2 = \delta$ . Since  $\delta > 1$  and  $0 \leq \tilde{W}_q$  are convex along lines parallel to  $\lambda_1 = 0$  and  $\lambda_2 = 0$ , therefore  $\tilde{W}_q = 0$  on edges connecting the vertexes  $(\pm\delta, \pm\delta)$  in the  $\sigma_1\sigma_2$  plane. Repeating the argument, we conclude that  $\tilde{W}_q = 0$  inside the square  $\Omega_0 = \{(\lambda_1, \lambda_2); \lambda_1 \leq \delta, \lambda_2 \leq \delta\}$ . So, for  $\delta$ -short maps  $W_q \equiv 0$ .

Since  $\tilde{W}_q(\lambda_1, \lambda_2)$  is even and convex in  $\lambda_2$ , it will attain its minimum with respect to  $\lambda_2$  only when  $\lambda_2 = 0$ . Denote by  $\tilde{W}^0(\lambda_1) = \min_{\lambda_2} \tilde{W}(\lambda_1, \lambda_2)$  when  $\lambda_1 > \delta$ . Suppose that  $\lambda^0(\lambda_1)$  is the largest

value of  $\lambda_2$  for which  $\tilde{W}_q(\lambda_1, \lambda^0) = \tilde{W}^0(\lambda_1)$ ,  $\lambda_1 > \delta$ . The convexity of  $\tilde{W}_q$  in  $\lambda_2$  implies that  $\tilde{W}_q(\lambda_1, \lambda_2) = \tilde{W}^0(\lambda_1)$  for  $\lambda_2 \leq \lambda^0(\lambda_1)$ ,  $\lambda_1 > \delta$ . In the same way, using the symmetry of  $\tilde{W}_q$  in its arguments, we will arrive at  $\tilde{W}_q(\lambda_1, \lambda_2) = \tilde{W}^0(\lambda_2)$  for  $\lambda_1 \leq \lambda^0(\lambda_2)$ ,  $\lambda_2 > \delta$ . Evidently, for the rest of deformation regimes,  $\tilde{W}$  is convex.

If we denote by  $\Omega_1 = \{(\lambda_1, \lambda_2); \lambda_1 > \delta, \lambda_2 \leq \lambda^0(\lambda_1)\}$  and  $\Omega_2 = \{(\lambda_1, \lambda_2); \lambda_1 \leq \lambda^0(\lambda_2), \lambda_2 > \delta\}$ , the ranges of principal stretches, corresponding to uniaxial tensions in directions of those stretches, respectively [51], we finally arrive at

$$\tilde{W}_q(\lambda_1, \lambda_2) = \begin{cases} 0, & \text{in } \Omega_0, \\ \tilde{W}^0(\lambda_1), & \text{in } \Omega_1, \\ \tilde{W}^0(\lambda_2), & \text{in } \Omega_2, \\ \tilde{W}(\lambda_1, \lambda_2), & \text{else.} \end{cases} \quad (42)$$

Besides opportunity of explicit relaxation, in [41] the derivation of criteria for convexity and quasi-convexity is described. In view of rank-one convexity,  $\tilde{W}_q$  satisfies Legendre-Hadamard inequality from which it follows

$$\tilde{W}_q^1 \geq 0, \quad \tilde{W}_q^2 \geq 0, \quad \tilde{W}_q^{11} \geq 0, \quad \tilde{W}_q^{22} \geq 0, \quad (43)$$

$$G \geq 0, \quad \sqrt{\tilde{W}_q^{11} \tilde{W}_q^{22}} - \tilde{W}_q^{12} \geq H - G, \quad \sqrt{\tilde{W}_q^{11} \tilde{W}_q^{22}} + \tilde{W}_q^{12} \geq -H - G. \quad (44)$$

For convexity of  $\tilde{W}_q$  in corresponding domain instead of the last two equalities, the stronger conditions

$$\tilde{W}_q^{11} \tilde{W}_q^{22} - (\tilde{W}_q^{12})^2 \geq 0, \quad G \geq |H|, \quad (45)$$

must be satisfied. Above

$$\tilde{W}_q^j = \frac{\partial \tilde{W}_q}{\partial \lambda_j}, \quad \tilde{W}_q^{jk} = \frac{\partial^2 \tilde{W}_q}{\partial \lambda_j \partial \lambda_k}, \quad G = \frac{\lambda_1 \tilde{W}_q^1 - \lambda_2 \tilde{W}_q^2}{\lambda_1^2 - \lambda_2^2}, \quad H = \frac{\lambda_2 \tilde{W}_q^1 - \lambda_1 \tilde{W}_q^2}{\lambda_1^2 - \lambda_2^2}. \quad (46)$$

The other way is the adding of pure bending contribution to the elastic energy of the tissue. Since actin-myosin network contraction leads to compressive or non-stretching stresses, we have to incorporate the elastic energy mainly for such deformations. According to Section 3 for non-stretching stresses, we have

i. (short deformations and compressive stresses)

$$\Gamma - \lim_{h \rightarrow 0} \frac{1}{h^\beta} E^{(h)} = 0 \quad \text{in the range } \beta \in \left[0, \frac{5}{3}\right), \quad (47)$$

ii. (isometric deformations, neither stretch nor compressive stresses)

$$\Gamma - \lim_{h \rightarrow 0} \frac{1}{h^2} E^{(h)} = E_b. \quad (48)$$

The deformation regime  $I \geq Id$  corresponding to tensile stresses leads to  $E_m[\mathbf{r}]$ , which is already lower semi-continuous. In the case of uniaxial tension, there is no bending and the energy expression will look like the middle rows of  $W_q$  (42). Thence, the total energy might be given as follows:

$$E[\mathbf{r}] = -\int_{\Omega} \mathbf{f} \cdot \mathbf{r} \, d\mathbf{x} + \begin{cases} 0, \mathbf{I} \leq \delta \, \text{Id}, \\ \frac{1}{2} \int_{\Omega} \tilde{W}^0(\lambda_1(\nabla \mathbf{r})) \, d\mathbf{x}, \text{ for uni-axial tension in the direction of } \lambda_1, \\ \frac{1}{2} \int_{\Omega} \tilde{W}^0(\lambda_2(\nabla \mathbf{r})) \, d\mathbf{x}, \text{ for uni-axial tension in the direction of } \lambda_2, \\ \frac{1}{24} \int_{\Omega} Q_2(\mathbf{II}) \, d\mathbf{x}, \mathbf{I} = \text{Id}, \\ \frac{1}{2} \int_{\Omega} W_q(\nabla \mathbf{r}) \, d\mathbf{x}, \text{ otherwise.} \end{cases} \quad (49)$$

We assume that the tissue is homogeneous and isotropic, so according to Remark 1

$$Q_2(\mathbf{II}) = 2\mu |\mathbf{II}|^2 + \frac{\lambda \cdot 2\mu}{\lambda + 2\mu} \text{tr}^2 \mathbf{II}. \quad (50)$$

Furthermore, the membrane energy density function we take in the following form [52, 53]:

$$W(\nabla \mathbf{r}) = \gamma_1 (I_1 - 3) + \gamma_2 (I_1 - 3)^2, \quad (51)$$

which is valid for large deformations of incompressible hyper-elastic membranes. Above,  $I_1 = \text{tr} \mathbf{I}$  is the first strain invariant,  $\gamma_1 > 0$  and  $\gamma_2 > 0$  are material parameters, evaluated experimentally in [53]. For a neo-Hookean material  $2\gamma_1 = \mu$  and  $2\gamma_2 = \kappa$ , in which  $\mu$  is the shear modulus and  $\kappa$  is the bulk modulus.  $\tilde{W}_q$  and  $\tilde{W}^0$  are determined according to the procedure described above. For that reason,  $I_1$  must be represented in terms of the principal stretches  $\lambda_1$  and  $\lambda_2$  as follows:

$$I_1(\lambda_1, \lambda_2) = \lambda_1^2 + \lambda_2^2 + \lambda_3^2 = \lambda_1^2 + \lambda_2^2 + \frac{1}{\lambda_1^2 \lambda_2^2}, \quad (52)$$

in which the incompressibility condition  $\lambda_1 \lambda_2 \lambda_3 = 1$  is taken into account.

For any fixed  $\lambda_1 > 1$  (uniaxial tension in the first principal direction), the corresponding  $\tilde{W}(\lambda_1, \lambda_2)$  attains its minimum with respect to  $\lambda_2$  at the maximal positive root of

$$\frac{\partial \tilde{W}}{\partial \lambda_2} = 2\lambda_2 \left( 1 - \frac{1}{(\lambda_1^2 + \lambda_2^2)^2} \right) [\gamma_1 + 2\gamma_2 (I_1 - 3)] = 0. \quad (53)$$

Since in the uniaxial tension regime  $\lambda_1^2 + \lambda_2^2 > 1$ , we finally get

$$\lambda^0(\lambda_1) = \frac{1}{\sqrt{\lambda_1}}. \quad (54)$$

Then,

$$W^0(\lambda_1) = \frac{1}{\lambda_1^2}(\lambda_1^3 - 3\lambda_1 + 2)[\gamma_1\lambda_1 + \gamma_2(\lambda_1^3 - 3\lambda_1 + 2)]. \quad (55)$$

The correspondent tension is defined by

$$\tau_1(\lambda_1) = \frac{\partial W^0(\lambda_1)}{\partial \lambda_1} = 2 \frac{\lambda_1^3 - 1}{\lambda_1^3} [\gamma_1\lambda_1 + 2\gamma_2(\lambda_1^3 - 3\lambda_1 + 2)]. \quad (56)$$

Since  $\tilde{W}$  is obviously symmetric in its arguments, in the case of uniaxial tension in the second principal direction, we would have

$$W^0(\lambda_2) = \frac{1}{\lambda_2^2}(\lambda_2^3 - 3\lambda_2 + 2)[\gamma_1\lambda_2 + \gamma_2(\lambda_2^3 - 3\lambda_2 + 2)], \quad (57)$$

and

$$\tau_2(\lambda_2) = \frac{\partial W^0(\lambda_2)}{\partial \lambda_2} = 2 \frac{\lambda_2^3 - 1}{\lambda_2^3} [\gamma_1\lambda_2 + 2\gamma_2(\lambda_2^3 - 3\lambda_2 + 2)]. \quad (58)$$

It is evident, that when we substitute  $\lambda_1 = 1$  in the first case and  $\lambda_2 = 1$  in the second case, we arrive at undeformed configuration of the membrane, so the relaxed energy is fully consistent.

Forces driving tissue deformation are strongly localized and in general are compressive. Force  $\mathbf{f}$  must possess those properties.



## 5. Finite element analysis of three-dimensional shape of some characteristic deformations of tissues during morphogenesis

In this section, we summarize main results of finite element analysis of a single layer tissue model, the elastic energy of which is given by

$$E[\mathbf{r}] = hE_m[\mathbf{r}] + h^3E_b[\mathbf{r}] \quad (59)$$

in which  $E_m$  and  $E_b$  are defined in Eqs. (49)–(51). Since the discretization procedure is standard, we omit the details and bring only the main results.

In **Figure 6**, we bring the model of a single-cell (element) and cell-cell junction (in red). All structures (plate and shell) considered in this section entirely consist of such cell groups. In all tissues considered below, the height of a cell  $h = 4r$  and  $h = 200d$ , in which  $r$  is its side and  $d$  is the diameter of actin fibres. The ratio of Young's moduli of a cell and actin fibres is  $E_{\text{act}} = 3E_{\text{cell}}$  and of actin fibres and cell-cell links  $E_{\text{act}} = 1.5E_{\text{link}}$ .

We consider

- i. initially flat rectangular plate (**Figure 7** (left)),
- ii. cylindrical shell (**Figure 9** (left)),
- iii. spherical shell (**Figure 11** (left)).



**Figure 6.** Single-cell model (left) and adherens junction model (right): diagonals of the top hexagon imitate actin fibres, red areas between cells imitate junction bonds.

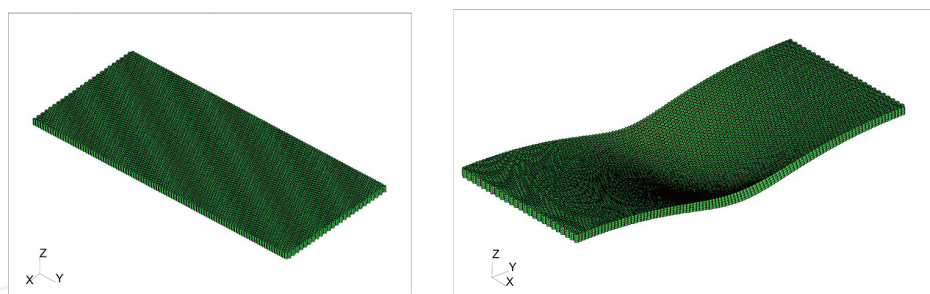


**Figure 7.** Apical constriction of initially flat tissue. It consists from 5050 elements or cells and has 529,245 DOFs.

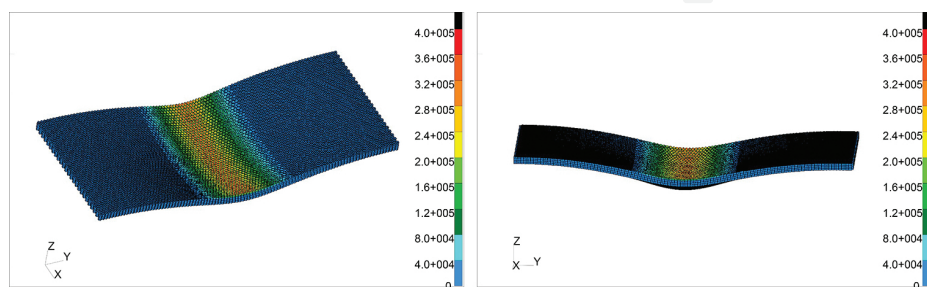


**Figure 8.** von Mises stress distribution in deformed configurations.

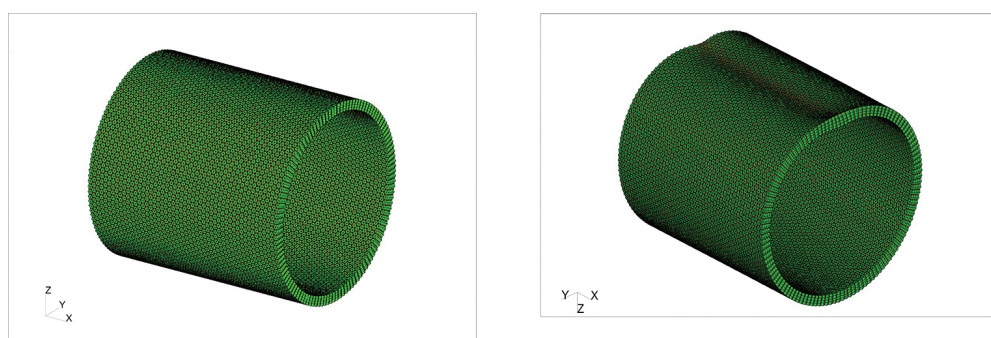


**Figure 9.** Apical constriction of initially cylindrical tissue. It consists from 5975 elements or cells and has 621,375 DOFs.

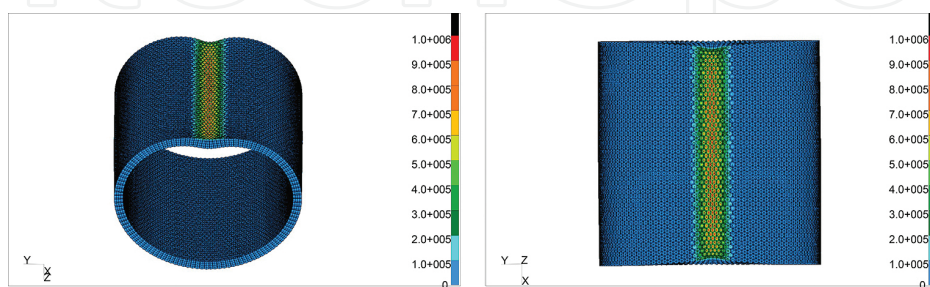


**Figure 10.** von Mises stress distribution in deformed configurations.

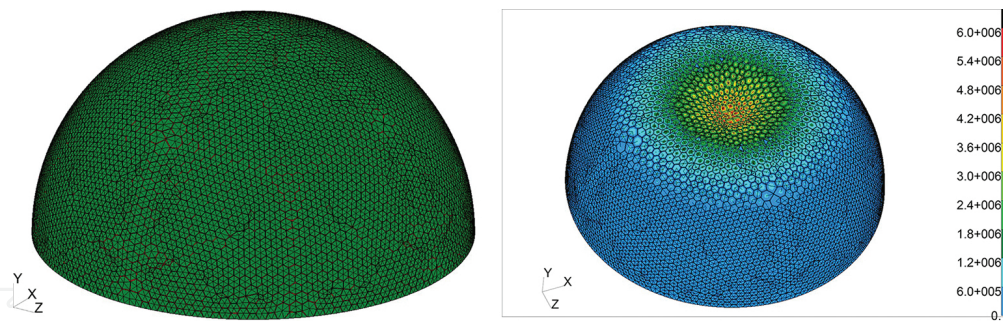


**Figure 11.** Apical constriction of initially spherical tissue. It consists from 3126 elements or cells and has 325,245 DOFs.

Elements of the middle part of the rectangular tissue are compressed in apical sides to imitate apical constriction in cells. Increasing the compressing stresses, the tissue is bent and a blaster-shaped pattern is formed as shown in **Figure 7** (right). The quantitative picture of the stresses arising in the tissue is drawn in **Figure 8**.

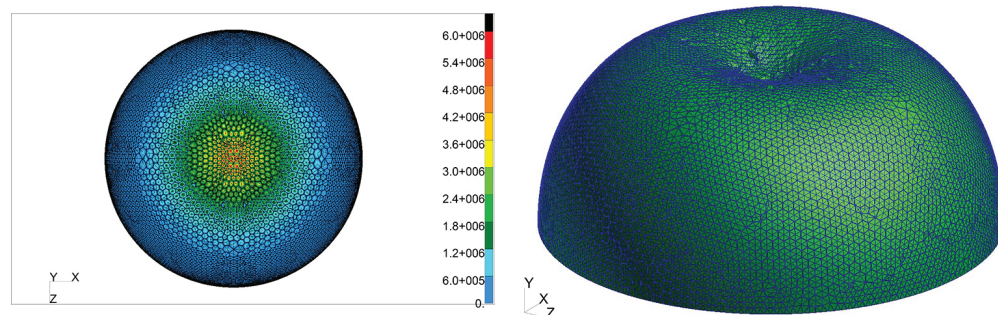


**Figure 12.** von Mises stress distribution in deformed configurations.

Next, we consider a cylindrical shell to imitate ventral furrow (generally all tubular patterns) formation. Elements of the top part of the cylinder are constrained in the apical sides by compressing the links standing for apical fibres (see **Figure 9**). Increasing the compressing stresses, the ventral furrow formation is simulated similar to stages presented in **Figure 1**. The quantitative picture of the stresses arising in the tissue is drawn in **Figure 10**.

Finally, a spherical shell is simulated. Cells at the top of a semi-sphere are constrained in apical sides and depending on values of compressing stresses various stages of blastopore formation in archenteron can be described (see **Figure 11** (right)). The quantitative picture of the stresses arising in the tissue is drawn in **Figure 12**.

## 6. Conclusions

Analysis based on lower semi-continuous energy functionals reveals real three-dimensional deformations of soft epithelial tissues. Having different forms for different deformation regimes, such as compressive stresses (short deformations), uniaxial tensions collinear to

principal directions of the first fundamental form, no stretching or pure bending stresses (isometric deformations) and stretching stresses (large deformations), the resulting total energy is lower semi-continuous, so the existence of its minimizers, that is, real deformations, is ensured. Particular energy density functions are chosen and the explicit form of the total energy functional is obtained, thereby the discretization is made easy.

On the basis of obtained energy functional, a three-dimensional discretized model of epithelial tissues undergoing combined stretching and bending deformations is constructed. Discretization elements correspond to single cells forming the tissue. Actin fibres and cell-cell adhesion links, mainly contributing on the tissue energy, are explicitly embedded in elements. Deformations characteristic to specific embryonic tissues (ventral furrow, neural tube, neurosphere) observed earlier are described quantitatively increasing contractile stresses in fibres.

## Dedication

We thankfully dedicate the chapter to the blessed memory of our good fellow and colleague, a candidate of physical and mathematical sciences, Hamlet V. Hovhannisyan (1956–2016), who unexpectedly died before he could realize his best scientific ideas.

## Acknowledgements

The theoretical part of the chapter is investigated under the guidance of Doctor, Professor Benedikt Wirth, Institute for Computational and Applied Mathematics, University of Münster, whom we are heartily thankful. The work of As. Kh. and S. O. was made possible in part by a research grant from the Armenian National Science and Education Fund (ANSEF) based in New York, NY, USA.

## Nomenclature

$\cdot$	Inner (dot) product
$\lambda, \mu$	Lamé coefficients
$\lambda_1, \lambda_2$	Principal stretches
$E_h$	Rescaled three-dimensional total energy
$\mu(\Omega)$	Measure of bounded open set $\Omega$
$\nabla$	Gradient (nabla) operator

$\Omega$	Midsurface of the epithelium
$\text{rank } \mathbf{F}$	Rank of the matrix $\mathbf{F}$
$\otimes$	Tensor product
dist	Usual distance in three-dimensional Euclidean space
$d$	Diameter of actin fibres
$E$	Three-dimensional elastic energy
$E_b$	Bending energy
$E_h$	Rescaled three-dimensional elastic energy
$E_m$	Membrane energy
$E_{act}$	Young's modulus of actin fibres
$E_{cell}$	Young's modulus of a cell
$E_{link}$	Young's modulus of cell-cell links
$h$	Thickness of the epithelium or a single cell
$r$	Side of a single cell
$W$	Membrane energy density function
$W_q$	The quasi-convex envelope of $W$
$\mathbf{II}$	The second fundamental form associated with deformation $\mathbf{r}$
$\mathbf{I}$	The first fundamental form associated with deformation $\mathbf{r}$
$\mathbf{n}$	Unit normal vector
$\mathbf{r}$	Deformation acting from $\mathbb{R}^2$ to $\mathbb{R}^3$
$\text{Id}_{2 \times 2}$	$2 \times 2$ identity matrix
$\text{SO}(3)$	The group of all rotations about the origin of three-dimensional Euclidean space

## Author details

Ara S. Avetisyan, Asatur Zh. Khurshudyan\* and Sergey K. Ohanyan

\*Address all correspondence to: [khurshudyan@mechins.sci.am](mailto:khurshudyan@mechins.sci.am)

Department of Dynamics of Deformable Systems and Connected Fields, Institute of Mechanics, National Academy of Sciences of Armenia, Yerevan, Armenia



## References

- [1] Rhumbler L., Zur Mechanik des Gastrulationsvorganges insbesondere der Invagination Eine entwickelungsmechanische Studie. *Archiv für Entwicklungsmechanik der Organismen*, 1902, vol. 14, issue 3, pp. 401–476.
- [2] Lewis W. H., Mechanics of invagination. *The Anatomical Record*, 1947, vol. 97, issue 2, pp. 139–156.
- [3] Odell G. M., Oster G., Alberch P., Burnside B., The mechanical basis of morphogenesis: I. Epithelial folding and invagination. *Developmental Biology*, 1981, vol. 85, issue 2, pp. 446–462.
- [4] Polyakov O., Bing H., Michael S., Joshua W. S., Matthias K., Wieschaus E., Passive mechanical forces control cell-shape change during *Drosophila* ventral furrow formation. *Biophysical Journal*, 2014, vol. 107, issue 4, pp. 998–1010.
- [5] Keller R., Developmental biology. Physical biology returns to morphogenesis. *Science*, 2012, vol. 338, pp. 201–203.
- [6] Mammoto T., Ingber D. E., Mechanical control of tissue and organ development. *Development*, 2010, vol. 137, pp. 1407–1420.
- [7] Martin A. C., Goldstein B., Apical constriction: themes and variations on a cellular mechanism driving morphogenesis. *Development*, 2014, vol. 141, pp. 1987–1998.
- [8] Sawyer J. M., Harrell J. R., Shemer G., Sullivan-Brown J., Roh-Johnson M., Goldstein B., Apical constriction: a cell shape change that can drive morphogenesis. *Developmental Biology*, 2010, vol. 341, pp. 5–19.
- [9] Martin A. C., Pulsation and stabilization: contractile forces that underlie morphogenesis. *Developmental Biology*, 2010, vol. 341, pp. 114–25.
- [10] Martin A. C., Kaschube B., Wieschaus E. F., Pulse contractions of an actin-myosin network drive apical constriction. *Nature*, 2009, vol. 457, issue 22, pp. 495–501.
- [11] Jones G. W., Chapman S. J., Modelling apical constriction in epithelia using elastic shell theory. *Biomechanics and Modeling in Mechanobiology*, 2010, vol. 9, issue 3, pp. 247–261.
- [12] Ciarletta P., Ben Amar M., Labouesse M., Continuum model of epithelial morphogenesis during *Caenorhabditis elegans* embryonic elongation. *Philosophical Transactions of the Royal Society A: Mathematical, Physical and Engineering Sciences*, 2009, vol. 367, pp. 3379–3400.
- [13] von Dassow M., Davidson L., Variation and robustness of the mechanics of gastrulation: the role of tissue mechanical properties during morphogenesis. *Birth Defects Research Part C: Embryo Today*, 2007, vol. 81, issue 4, pp. 253–269.

- [14] Du. X., Osterfield M., Shvartsman S. Y., Computational analysis of three-dimensional epithelial morphogenesis using vertex models. *Physical Biology*, 2014, vol. 11, issue 6, 15 p.
- [15] Fletcher A. G., Osterfield M., Baker R. E., Shvartsman S. Y., Vertex models of epithelial morphogenesis. *Biophysical Journal*, 2014, vol. 106, issue 11, pp. 2291–2304.
- [16] Imai M., Furusawa K., Mizutani T., Kawabata A., Haga H., Three-dimensional morphogenesis of MDCK cells induced by cellular contractile forces on a viscous substrate. *Scientific Reports*, 2015, vol. 5, 14208.
- [17] Ingber D. E., Mechanical control of tissue morphogenesis during embryological development. *International Journal of Developmental Biology*, 2006, vol.50, pp. 255–266.
- [18] Inoue Y., Suzuki M., Watanabe T., Yasue N., Tateo I., Adachi T., Ueno N., Mechanical roles of apical constriction, cell elongation, and cell migration during neural tube formation in *Xenopus*. *Biomechanics and Modeling in Mechanobiology*, 2016, DOI 10.1007/s10237-016-0794-1.
- [19] Jauvert S., Peyroux R., Richefeu V., A mechanical model for cell motility and tissue morphogenesis. *Computer Methods in Biomechanics and Biomedical Engineering*, 2013, vol. 16, pp. 13–14.
- [20] Lecuit T., Lenne P.-F., Cell surface mechanics and the control of cell shape, tissue patterns and morphogenesis. *Nature Reviews Molecular Cell Biology*, 2007, vol. 8, pp. 633–644.
- [21] Murisic N., et al., From discrete to continuum models of three-dimensional deformations in epithelial sheets. *Biophysical Journal*, 2015, vol. 109, issue 1, pp. 154–163.
- [22] Patwari P., Lee R. T., Mechanical control of tissue morphogenesis. *Circulation Research*, 2008, vol. 103, pp. 234–243.
- [23] Rauzi M., Krzic U., Saunders T. E., Krajnc M., Zihlerl P., Hufnagel L., Leptin M., Embryo-scale tissue mechanics during *Drosophila* gastrulation movements. *Nature Communications*, 2015, vol. 6, Article number: 8677, doi: 10.1038/ncomms9677.
- [24] Siedlik M. J., Nelson C. M., *Mechanics of tissue morphogenesis*. In “*Cell and Matrix Mechanics*” edited by Kaunas R., Zemel A., CRC Press, 2014.
- [25] Vaughan B. L. Jr., Baker R. E., Kay D., Maini P. K., A modified Oster-Murray-Harris mechanical model of morphogenesis. *SIAM Journal of Applied Mathematics*, 2013, vol. 73, issue 6, pp. 2124–2142.
- [26] Wyczalkowski M. A., Chen Z., Filas B. A., Varner V. D., Taber L. A., Computational models for mechanics of morphogenesis. *Birth Defects Research Part C: Embryo Today: Reviews*, 2012. vol. 96, issue 2, pp. 132–152.
- [27] Hannezo E., Prost J., Joanny J.-F., Theory of epithelial sheet morphology in three dimensions. *PNAS*, vol. 111, issue 1, pp. 27–32.

- [28] Dacorogna B., *Direct Methods in the Calculus of Variations*. Springer, 2009.
- [29] Dal Maso G., *An Introduction to  $\Gamma$ -Convergence*. Birkhäuser, Boston, 1993.
- [30] Steigman D. J., Pipkin A. C., Finite deformations of wrinkled membranes. *Quarterly Journal of Mechanics and Applied Mathematics*, 1989, vol. 42, pp. 427–440.
- [31] Kohn R. V., Strang G., Optimal design and relaxation of variational problems I, II, III. *Communications on Pure and Applied Mathematics*, 1986, vol. 39, pp. 1–25 (I), 139–182 (II), 353–377 (III).
- [32] Hilgers M. G., Pipkin A. C., Elastic sheets with bending stiffness. *Quarterly Journal of Mechanics and Applied Mathematics*, 1992, vol. 45, issue 1, pp. 57–75.
- [33] Hilgers M. G., Pipkin A. C., Bending energy of highly elastic membranes. *Quarterly of Applied Mathematics*, 1992, vol. L, issue 2, pp. 389–400.
- [34] Hilgers M. G., Pipkin A. C., Bending energy of highly elastic membranes II. *Quarterly of Applied Mathematics*, 1996, vol. LIV, issue 2, pp. 307–316.
- [35] Hilgers M. G., Pipkin A. C., Energy-minimizing deformations of elastic sheets with bending stiffness. *Journal of Elasticity*, 1993, vol. 31, pp. 125–139.
- [36] Hilgers M. G., Pipkin A. C., The Graves condition for variational problems of arbitrary order. *IMA Journal of Applied Mathematics*, 1992, vol. 48, pp. 265–269.
- [37] Schmidt B., Fraternali F., Universal formulae for the limiting elastic energy of membrane networks. *Journal of the Mechanics and Physics of Solids*, 2012, vol. 60, pp. 172–180.
- [38] Meyers N. G., Quasi-convexity and lower semi-continuity of multiple variational integrals of any order. *Transactions of AMS*, 1965, vol. 119, pp. 125–149.
- [39] Dal Maso G., Fonseca I., Leoni G., Morini M., Higher-order quasi-convexity reduces to quasi-convexity. *Archive for Rational Mechanics and Analysis*, 2004, vol. 171, pp. 55–81.
- [40] Cagnetti F.,  $k$ -Quasi-convexity reduces to quasi-convexity. *Proceedings of the Royal Society of Edinburgh: Section A Mathematics*, 2011, vol. 141, issue 4, pp. 673–708.
- [41] Pipkin A. C., The relaxed energy density for isotropic elastic membranes. *IMA Journal of Applied Mathematics*, 1986, vol. 36, pp. 85–99.
- [42] Pipkin A. C., Relaxed energy densities for large deformations of membranes. *IMA Journal of Applied Mathematics*, 1994, vol. 52, pp. 297–308.
- [43] Ciarlet P. G., *Mathematical Elasticity*, in 3 vol. Elsevier, 1993.
- [44] Friesecke G., James R. D., Muller S., A hierarchy of plate models derived from nonlinear elasticity by Gamma-convergence. *Archive for Rational Mechanics and Analysis*, 2006, vol. 180, pp. 183–236.

- [45] Le Dret H., Raoult A., The nonlinear membrane model as variational limit of nonlinear three-dimensional elasticity. *Journal de Mathématiques Pures et Appliquées*, 1995, vol. 74, pp. 549–578.
- [46] Conti S., Maggi F., Confining thin elastic sheets and folding paper. *Archive for Rational Mechanics and Analysis*, 2008, vol. 187, pp. 1–48.
- [47] Friesecke G., James R. D., Muller S., A theorem on geometric rigidity and the derivation of nonlinear plate theory from three-dimensional elasticity. *Communications on Pure and Applied Mathematics*, 2002, vol. 55, issue 11, pp. 1461–1506.
- [48] Friesecke G., James R. D., Mora M. G., Muller S., Derivation of nonlinear bending theory for shells from three-dimensional nonlinear elasticity by  $\Gamma$ -convergence. *Comptes Rendus de l'Académie des Sciences. Series I Mathematics*, 2003, vol. 336, pp. 697–702.
- [49] Kirchhoff G., Über das Gleichgewicht und die Bewegung einer elastischen Scheibe. *Journal für die reine und angewandte Mathematik*, 1850, vol. 40, pp. 51–88.
- [50] Pipkin A. C., Elastic materials with two preferred states. *Quarterly Journal of Mechanics and Applied Mathematics*, 1991, vol. 44, issue 1, pp. 1–15.
- [51] Cesana P., Plucinsky P., Bhattacharya K., Effective behavior of nematic elastomer membranes. *Archive for Rational Mechanics and Analysis*, 2015, vol. 218, issue 2, pp. 863–905.
- [52] Chagnon G., Rebouah M., Favier D., Hyperelastic energy densities for soft biological tissues: a review. *Journal of Elasticity*, 2015, vol. 120, pp. 129–160.
- [53] Raghavan M.L., Vorp D. A., Toward a biomechanical tool to evaluate rupture potential of abdominal aortic aneurysm: Identification of a finite strain constitutive model and evaluation of its applicability. *Journal of Biomechanics*, 2000, vol. 33, issue 4, pp. 475–482.

